

# Enzymology, Structure, and Dynamics of Acetohydroxy Acid Isomeroreductase

RENAUD DUMAS,\*<sup>†</sup> VALÉRIE BIOU,<sup>‡</sup>  
FRÉDÉRIC HALGAND,<sup>§</sup> ROLAND DOUCE,<sup>†</sup> AND  
RONALD G. DUGGLEBY<sup>#</sup>

Laboratoire Mixte CNRS/INRA/Aventis, Aventis CropScience,  
14-20 rue Pierre Baizet, 69263 Lyon, France, Institut de  
Biologie Structurale, 41 rue Jules Horowitz,  
38027 Grenoble, France, Institut de Chimie des  
Substances Naturelles, Avenue de la Terrasse,  
91198 Gif-sur-Yvette, France, and Centre for Protein  
Structure, Function and Engineering, Department of  
Biochemistry, University of Queensland,  
Brisbane, QLD 4072, Australia

Received December 6, 2000

## ABSTRACT

Acetohydroxy acid isomeroreductase is a key enzyme involved in the biosynthetic pathway of the amino acids isoleucine, valine, and leucine. This enzyme is of great interest in agrochemical research because it is present only in plants and microorganisms, making it a potential target for specific herbicides and fungicides. Moreover, it catalyzes an unusual two-step reaction that is of great fundamental interest. With a view to characterizing both the mechanism of inhibition by potential herbicides and the complex reaction mechanism, various techniques of enzymology, molecular biology, mass spectrometry, X-ray crystallography, and theoretical simulation have been used. The results and conclusions of these studies are described briefly in this paper.

## Introduction

The pathway for the biosynthesis of the branched-chain amino acids involves several unusual reactions and enzymes. The enzymes (acetohydroxy acid synthase, EC 4.1.3.18; acetohydroxy acid isomeroreductase, EC 1.1.1.86; and dihydroxy acid dehydratase, EC 4.2.1.9) that catalyze the first three steps required for the synthesis of valine are also involved in the synthesis of isoleucine and leucine. One of the most remarkable of these enzymes is acetohydroxy acid isomeroreductase (AHIR; also known as

ketol-acid reductoisomerase, KARI), which catalyzes the reaction shown in Figure 1. The substrates are either 2-acetolactate (AL) or 2-aceto-2-hydroxybutyrate (AHB), and the two alternative products act as precursors of valine and leucine, or isoleucine, respectively.

This reaction is unusual in a number of ways. First, it involves an alkyl migration of a type found usually in cobalamin-dependent enzymes; however, the enzyme does not require this cofactor. Second, the alkyl migration is followed by a reduction; that these two dissimilar reactions occur in sequence is illustrated by the fact that the expected intermediate 3-hydroxy-3-methyl-2-oxobutyrate (HMOB intermediate from AL; Figure 1) can act as a substrate in the reductive reaction.<sup>1</sup> Third, the enzyme has an absolute requirement for Mg<sup>2+</sup>, and no other metal ion will substitute effectively. Metal ion-dependent dehydrogenases are not unusual, but a specific requirement for Mg<sup>2+</sup> is, as far as we are aware, unique. And last, the enzyme requires two bound metal ions for catalysis to occur.<sup>2</sup>

In this paper we will describe the biochemical and structural features of AHIR, with special emphasis on the plant enzyme for which the structure has been determined.<sup>3</sup>

## Occurrence and Subcellular Location

AHIR activity has been observed in bacteria, fungi, and plants, but not in animals. A number of AHIR gene and protein sequences may be found in various databases, although the only evidence that most of these are actually AHIR is their homology with the few examples that have been characterized biochemically.

The enzyme from plants, bacteria, and fungi is encoded by a single gene in each organism. The expression of the *Escherichia coli* enzyme is induced by the binding of either AL or AHB to a positive activator encoded by the gene *ilvY*.<sup>4,5</sup> In yeast, expression of AHIR is under general control and amino acid-specific regulation.<sup>6</sup> The fungal<sup>6</sup> and plant<sup>7–10</sup> enzymes are encoded by one nuclear gene per haploid genome, and the proteins are translocated into mitochondria or plastids, respectively. In the anaero-

Renaud Dumas was born in 1963 in Marseille, France. In 1991, he obtained his Ph.D. from the University of Grenoble and joined the Centre National de la Recherche Scientifique (CNRS). His research interests include plant metabolism and protein structure–function relationships.

Valérie Biou was born in Paris in 1962. She obtained her Ph.D. from the University Pierre et Marie Curie in Paris in 1989. She did postdoctoral work at the EMBL Grenoble outstation, at the Brookhaven National Laboratory, and at the Institut de Biologie Structurale de Grenoble. She has held a CNRS position since 1996. Her scientific interests range from the application of the anomalous signal to protein crystallography to structural studies of plant enzymes.

Frédéric Halgand was born in 1968 in France. He received his Ph.D. in biology from the University of Grenoble (1998), studying the application of mass spectrometry to biochemistry. He has held a CNRS position since 1998. His main interest is in biological mass spectrometry concerning the study of structure–function relationships of proteins, extending the use of H/D exchange that formed his Ph.D. studies, and more recently to the study of noncovalent complexes.

\* To whom correspondence and reprint requests should be addressed.  
E-mail: renaud.dumas@aventis.com. Telephone: 334 72 85 22 96. Fax: 334 72 85 22 97.

<sup>†</sup> Aventis CropScience.

<sup>‡</sup> Institut de Biologie Structurale.

<sup>§</sup> Institut de Chimie des Substances Naturelles.

<sup>#</sup> University of Queensland.

Roland Douce was born in France (1939) and obtained his Ph.D. in Paris (Sorbonne, 1969). He is currently Professor in Plant Biochemistry at the University of Grenoble, a member of the French Academy of Sciences (1996), and a foreign member of the National Academy of Sciences of the USA (1997). His interests center around general metabolism in higher plants.

Ron Duggleby was born in England (1945) and obtained his Ph.D. in Canada (Queen's University, 1972) before moving to Australia in 1975. He is currently Reader in Biochemistry at the University of Queensland. His interests are focused on the structure and mechanism of enzymes, particularly those that use thiamin diphosphate as a cofactor.

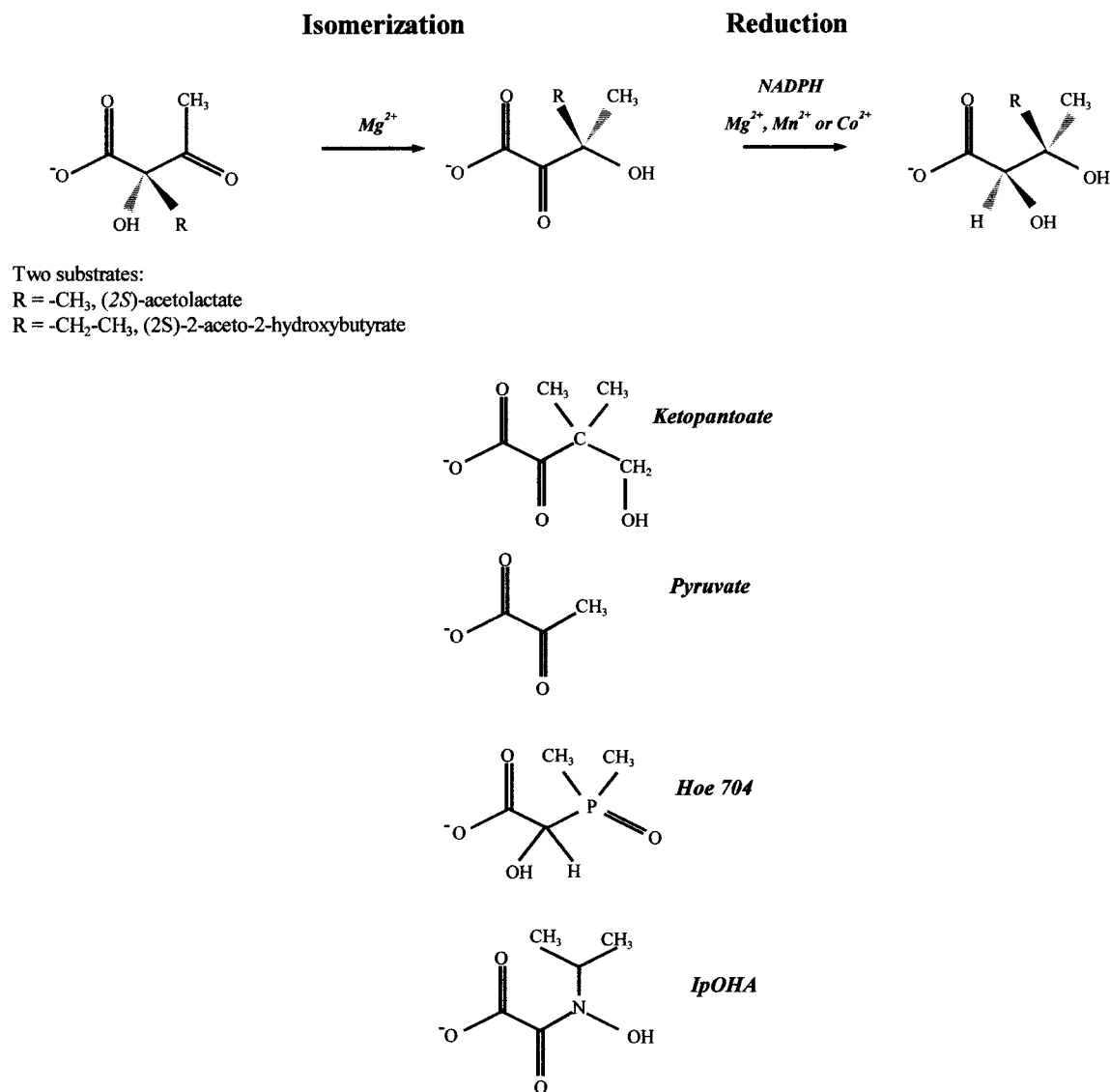


**FIGURE 1.** Reaction catalyzed by AHIR, reaction intermediate analogues (ketopantoate and pyruvate), and inhibitors (Hoe 704 and IpOHA). The substrates, (2*S*)-acetolactate or (2*S*)-2-aceto-2-hydroxybutyrate, are converted via an alkyl migration (isomerization) followed by a NADPH-dependent reduction to give (2*R*)-2,3-dihydroxy-3-isovalerate or (2*R*,3*R*)-2,3-dihydroxy-3-methylvalerate, respectively.

bic eucaryote *Piromyces* sp. E2, which lacks mitochondria, the enzyme is cytoplasmic.<sup>11</sup> Curiously, the yeast enzyme has a second function unrelated to its catalytic activity, acting to stabilize mitochondrial DNA<sup>12</sup>. The mechanism of stabilization, and the reason that AHIR is used to effect this function, are still unknown. This is, of course, not the only instance of enzymes having second functions unrelated to their catalytic properties. Other examples include aldehyde dehydrogenase, transketolase, and glutathione S-transferase acting as lens crystallins,<sup>13</sup> pyruvate decarboxylase forming fungal cytoplasmic filaments,<sup>14</sup> and the roles of glyceraldehyde 3-phosphate dehydrogenase in several processes.<sup>15</sup>

## Catalytic Properties

As mentioned earlier, the natural substrates of AHIR are AL and AHB, with an absolute specificity for the *S* isomer of both substrates (Figure 1), as demonstrated for the bacterial<sup>16–18</sup> and plant<sup>19</sup> enzymes. AHIR possesses similar

$K_m$  values for AL and AHB but a 5- to 8-fold higher activity with AHB compared to that with AL.<sup>7,20</sup> This property is important for the regulation of the flux leading to the different branched chain amino acids, since AHIR will favor the synthesis of the intermediate leading to isoleucine. In turn, isoleucine controls its own synthesis by inhibiting threonine deaminase, the only enzyme of the pathway that is unique to isoleucine biosynthesis.<sup>21</sup>

The reduction step requires transfer of the *pro-S* hydrogen atom from NADPH.<sup>20</sup> AHIR has a strong preference for NADPH ( $K_m$  from 2 to 15  $\mu\text{M}$ ) over NADH ( $K_m$  from 100 to 600  $\mu\text{M}$ ).<sup>7,22,23</sup> The nucleotide specificity of *E. coli* AHIR has been reversed using site-directed mutagenesis<sup>23</sup> by changing the amino acids involved in the binding of the 2'-phosphate of NADPH.<sup>24</sup> Unlike the bacterial enzyme, plant AHIR is strongly inhibited by NADP<sup>+</sup>, with a  $K_i$  of 5  $\mu\text{M}$ .<sup>7</sup>

AHIR has an absolute requirement for Mg<sup>2+</sup>, and no other divalent metal ion will substitute in the *E. coli*

enzyme.<sup>1</sup> The spinach enzyme<sup>2,25</sup> has traces of activity (~3%) with Mn<sup>2+</sup> and Co<sup>2+</sup>. Both the alkyl migration and the reduction require a metal ion. However, the stringency of metal requirement is restricted to the alkyl migration. The reduction step can utilize Mg<sup>2+</sup>, Mn<sup>2+</sup>, or Co<sup>2+</sup> equally well, as demonstrated by providing the HMOB intermediate or ketopantoate.<sup>1,2</sup> It was shown later by site-directed mutagenesis<sup>2</sup> and crystal structure determination<sup>3</sup> that this differential metal requirement is due to the existence of two distinct metal ion sites in the enzyme. The plant enzyme possesses a high affinity for magnesium ( $K_m$  of 5  $\mu\text{M}$ ) compared to its bacterial and fungal counterparts, which have  $K_m$  values of 400–900  $\mu\text{M}$ .<sup>2</sup> Lowered affinity for Mg<sup>2+</sup> of the plant enzyme has been described for a chimeric bifunctional enzyme composed of *Spinacia oleracea* AHIR and *Arabidopsis thaliana* acetohydroxy acid synthase<sup>26</sup> and also for a monomeric mutant of the *S. oleracea* AHIR.<sup>27</sup> Surprisingly, the enzyme from *Triticum aestivum* does not require added magnesium ions for activity and behaves as a monomer.<sup>28</sup>

There is no obvious reason that the alkyl migration and reduction reactions should occur in one enzyme. The intermediate resulting from the alkyl migration is not notably unstable,<sup>1</sup> nor is there any obvious alternative metabolic fate into which it might be diverted. Thus, there is no apparent reason that it needs to be trapped in the active site prior to reduction. Of course, using a single protein to perform the successive reactions may offer some small metabolic economy and a selective advantage that would be fixed during evolution. However, this argument could be applied equally to enzymes catalyzing most sequential metabolic reactions, and yet, for the most part, separate enzymes are utilized.

While it is generally accepted that the AHIR reaction occurs in two stages, the formation of the expected intermediate has never been shown directly. For example, Arfin and Umbarger<sup>20</sup> detected none of this intermediate and also showed that there was no equilibration of the intermediate with that added to reaction mixtures. While these results suggest that the intermediate is tightly bound, it remains a possibility that there is direct reduction during alkyl transfer so that the intermediate is never actually formed as a discrete entity. Under this interpretation, any activity toward added HMOB would represent a side reaction.

In addition to reducing presumed intermediates of the reaction such as HMOB, AHIR will also reduce analogues of this compound such as ketopantoate<sup>2,29</sup> (Figure 1) and pyruvate<sup>30</sup> (Figure 1). The former compound is an intermediate in pantothenate biosynthesis, and it was suggested originally that AHIR functions in this pathway in *Salmonella typhimurium*.<sup>29</sup> The question about the involvement of AHIR in pantothenate biosynthesis is complex since at least three enzymes, ketopantoate reductase,<sup>31</sup> oxopantoyl lactone reductase,<sup>32</sup> and AHIR,<sup>2,29</sup> would be required in this pathway. However, Shimizu et al.<sup>31</sup> showed the existence in *Pseudomonas maltophilia* 845 of an entirely separate reductase. That this ketopantoate reductase is responsible for the synthesis of D-(–)-pantoic

acid in *P. maltophilia* 845 is indicated by the observation that only this enzyme (and not ketopantoyl lactone reductase or AHIR) is missing in D-(–)-pantoate (or pantothenate)-requiring mutants.<sup>31</sup> It is of interest that the specific activity of this ketopantoate reductase toward HMOB is 8-fold higher than that of AHIR itself, showing that chemistry alone is not rate-limiting in HMOB reduction by AHIR. Evidently, creating an active site in AHIR that combines the isomerase and reductase activities has compromised the efficiency of the latter. This observation throws further doubt on the argument that using a single protein to perform the successive reactions may offer a selective advantage.

## Mechanisms of Inhibition

The enzyme is inhibited by a number of substances, including substrate analogues such as 2-methylactate and 3-aminopyridine-NADP<sup>+</sup>, divalent metal ions such as Mn<sup>2+</sup>, and reaction products.<sup>1,19,20,33</sup> However, the most interesting inhibitors are the reaction intermediate analogues 2-dimethylphosphinoyl-2-hydroxyacetate<sup>34</sup> (Hoe 704, Figure 1) and *N*-hydroxy-*N*-isopropylloxamate<sup>35</sup> (IpOHA, Figure 1). These two compounds behave as nearly irreversible inhibitors of AHIR. Both inhibitors are competitive with the carbon substrate and show a time-dependent increase in potency, due to the slow formation of a tightly bound enzyme–inhibitor complex.<sup>35,36</sup>

Due to the potent inhibition, coupled with the fact that AHIR is not present in animals, these compounds have attracted attention as potential herbicides. Hoe 704 binds to the plant enzyme 10-fold faster than IpOHA (association rate constants of  $22 \times 10^3 \text{ M}^{-1} \text{ s}^{-1}$  compared to  $1.9 \times 10^3 \text{ M}^{-1} \text{ s}^{-1}$ ) and acts as a better herbicide than IpOHA by a factor of 10.<sup>36</sup> Although both are lethal to plants, the concentrations needed to achieve a herbicidal effect are much higher than the *in vitro* studies on AHIR would suggest. It was proposed that the association rate of these compounds to the plant enzyme is correlated with their herbicidal potency, and that the reason for their weak activity is their slow-binding and competitive behavior. This latter feature is of particular importance since the apparent  $K_m$  of the plant enzyme for its substrate is quite low (approximately 10  $\mu\text{M}$ ), and partial inhibition of AHIR will cause the carbon substrate to accumulate rapidly, preventing further inhibition by competition.<sup>37</sup>

These studies suggest that an effective herbicide targeting this enzyme has to be either a competitive inhibitor with a high association rate or a noncompetitive inhibitor.<sup>37</sup> Compounds such as thiadiazole derivatives that are strong noncompetitive inhibitors of the plant enzyme were found by high-throughput screening.<sup>38</sup> However, none of these compounds selected *in vitro* behave as efficient inhibitors *in vivo*.

## Sequences and Conserved Residues

As mentioned earlier, there are a number of AHIR sequences in various databases, and analysis of these sequences has identified some common features as well

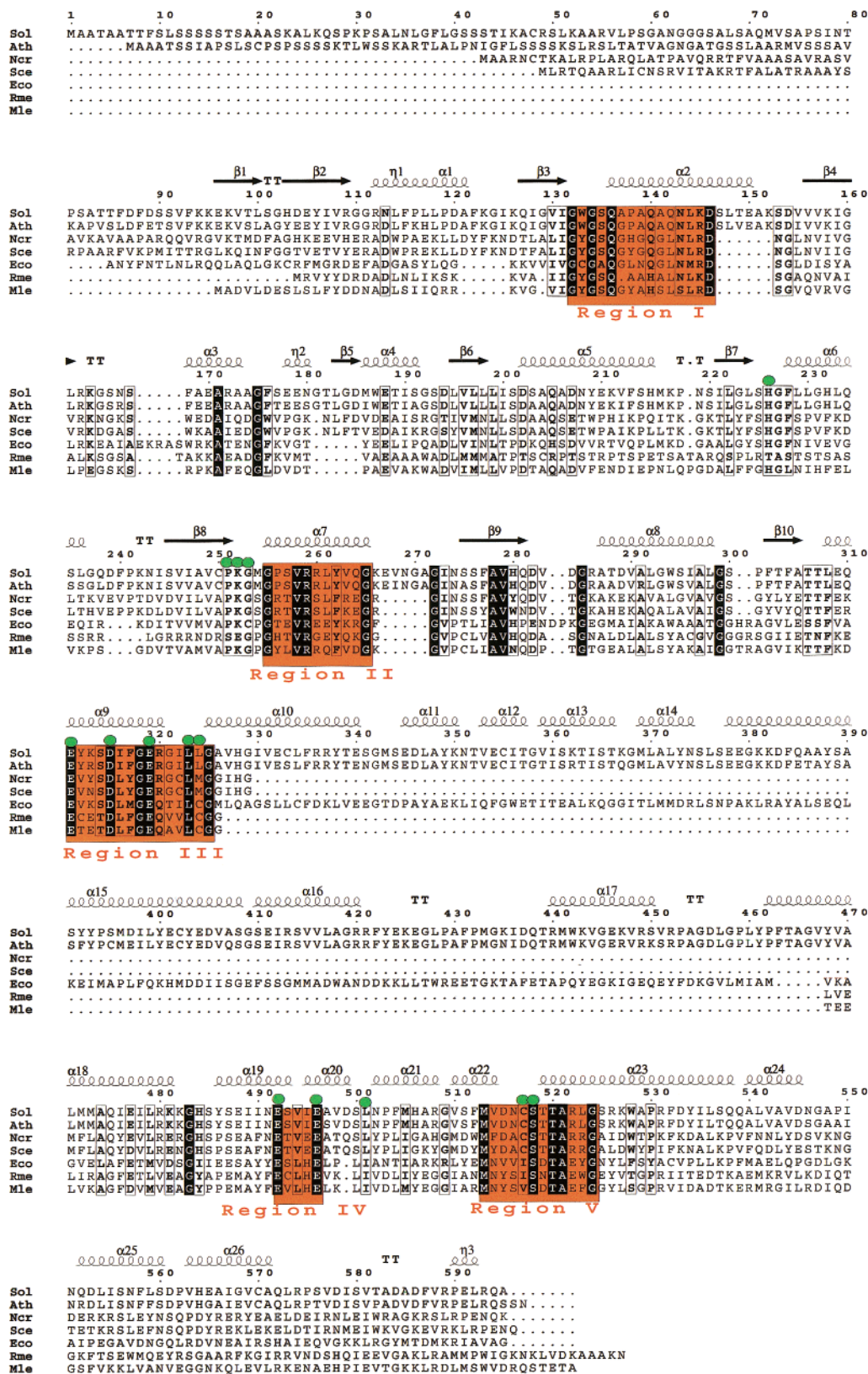


**FIGURE 2.** Alignment of representative AHIR amino acid sequences. The alignment was prepared using the program ESPrit;<sup>39</sup> boxes indicate conserved residues, using a threshold of 0.20 with the BLOSUM62 matrix.<sup>40</sup> The secondary structures ( $\alpha$  =  $\alpha$ -helix,  $\beta$  =  $\beta$ -sheet,  $\eta$  =  $3_{10}$ -helix, and T = turn) were calculated using the program DSSP<sup>41</sup> from the AHIR coordinates and are numbered sequentially. Orange boxes indicate regions I–V, and green circles indicate the positions of active site residues. Species abbreviations used: Sol, *Spinacia oleracea*; Ath, *Arabidopsis thaliana*; Sce, *Saccharomyces cerevisiae*; Ncr, *Neurospora crassa*; Eco, *Escherichia coli*; Rme, *Rhizobium meliloti*; and Mle, *Mycobacterium leprae*.

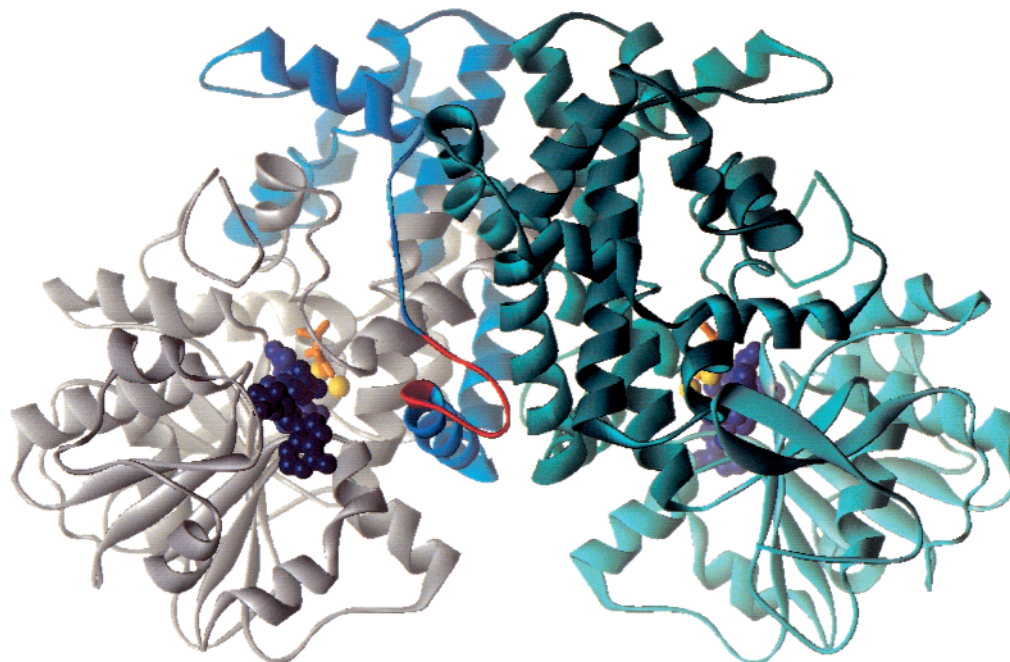


**FIGURE 3.** Ribbon representation of the spinach AHIR dimer (redrawn from Biou et al.<sup>3</sup>). The two monomers are shown complexed with NADPH (purple),  $Mg^{2+}$  (yellow), and the inhibitor IpOHA (orange). In the green monomer (right), the N-terminal domain interacting with NADPH is shown in light color while the C-terminal domain involved in the binding of  $Mg^{2+}$  and the inhibitor is in dark color. In the gray monomer (left), the insertion sequence and the loop involved in the dimerization of the spinach enzyme are indicated in blue and red, respectively.

as some important differences. Dumas et al.<sup>2</sup> analyzed eight AHIR sequences, and their conclusions are borne out by a more recent examination of 34 sequences (Duggleby, unpublished). An alignment of seven representative sequences is shown in Figure 2. There are five conserved regions (labeled I to V), and the first of these contains a typical GXGXX(G/A)XXX(G/A) motif, involved in the binding of the diphosphate bridge of the nucleotide of NAD(P)H-dependent dehydrogenases.<sup>8,24</sup> The functions of regions II–V were shown, by site-directed mutagenesis, to be involved in the active site.<sup>2</sup> Furthermore, this study demonstrated that region III and IV are involved in the binding of two metal ions required in the two steps of the reaction.

The plant and fungal enzymes possess an N-terminal extension that is not found in bacterial AHIR sequences. This is undoubtedly an organelle-targeting peptide that ensures that the enzyme is translocated correctly to plastids in plants and to mitochondria in fungi. More puzzling is an insert of approximately 140 residues in the middle of the plant enzymes. This is not found in fungal AHIR or that from most bacteria. However, in AHIR from *E. coli* and its close relatives such as *S. typhimurium* and *Haemophilus influenzae*, an insert having no sequence relationship with plant AHIR is also present. As will be discussed later, determination of the structure of the spinach enzyme indicated that this sequence is involved in the dimerization of the plant enzyme.<sup>3</sup>

## Structure Description

Overproduction of the mature spinach enzyme in *E. coli*<sup>19</sup> allowed purification of sufficient amounts of protein to

begin crystallization trials. Despite many attempts, no crystals suitable for diffraction analyses were obtained with the free enzyme. In contrast, the enzyme crystallizes well in the combined presence of an inhibitor (either Hoe 704 or IpOHA),  $Mg^{2+}$ , and NADPH.<sup>42</sup> Using these crystals, the structure of the spinach AHIR complexed with IpOHA,  $Mg^{2+}$ , and NADPH was determined at 1.65 Å resolution<sup>3</sup> (PDB code 1YVE). Later, attempts to crystallize the enzyme with its substrate AHB,  $Mn^{2+}$ , and NADPH led to the determination of the structure at 1.60 Å resolution of a second complex involving the metal ion, (phospho)-ADP-ribose, and dihydroxymethyl valerate, the reaction product<sup>25</sup> (PDB code 1QMG). The overall structure is the same in both complexes.

Figure 3 shows the active dimer with bound ligands. Each monomer is composed of two sequential domains. The N-terminal domain (residues 72–307) has a mixed  $\alpha/\beta$  structure with a classical dinucleotide binding fold (Rossmann fold). It contains most of the NADPH binding site, with the exception of the nicotinamide moiety, which is at the interface with the other domain (Figure 3). The C-terminal domain (residues 308–595), composed mostly of  $\alpha$ -helices structured in a barrel, has two functions. First, it contributes to the formation of the metal ion and substrate (analogue/inhibitor) recognition sites (Figure 3). Second, it is responsible for monomer–monomer interactions (Figure 3). Recently, Taylor<sup>43</sup> showed the presence of a knot in the C-terminal domain of AHIR. This was one of only five knotted proteins found in the entire protein structure data bank, and it shows the most complex geometry. The knot links two parts of the protein consisting of four helices each (residues 325–453 and 466–475).

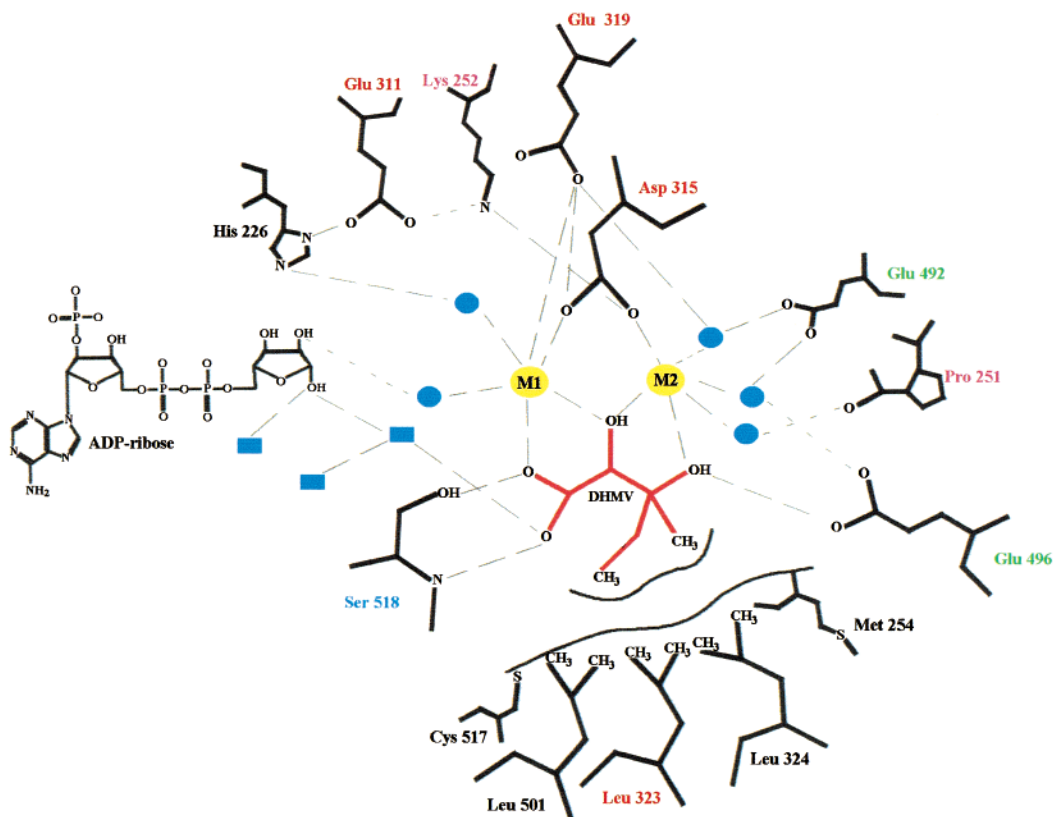


**FIGURE 4.** Active site of spinach AHIR complexed with 2,3-dihydroxy-3-methylvalerate (orange),  $Mn^{2+}$  (yellow), and (phospho)-ADP-ribose (black) (redrawn from Thomazeau et al.<sup>25</sup>). The dotted lines show electrostatic interactions within the active site. Most of the residues involved in ligand binding belong to the conserved regions as described in the text and are colored as follows: region II, pink; region III, red; region IV, green; and region V, blue. Nonconserved residues are shown in black. His226 is conserved except in the *Rhizobium meliloti* enzyme. Other residues that are not universally conserved are Met254, Leu324, Leu501, and Cys517. Water molecules involved in the active site are shown in blue. Water molecules observed only in the complex with (phospho)-ADP-ribose are shown as rectangles.

Those two regions superimpose closely in three dimensions. The question of how this knot forms during protein folding is still open.

The active site sits at the interface between the two domains of one monomer. It contains two divalent cations, five water molecules, one inhibitor or reaction product, and the nicotinamide moiety of the NADPH (Figures 3 and 4). As shown in Figure 4, the active site is very tightly packed, and the divalent cations interact closely with the inhibitor/product molecule, which explains the high recognition specificity and the need for an ordered access of the molecules. As will be discussed later, the active site is able to bind the carbon substrate or analogue only in the presence of the cofactors. In addition, the acceptance of two substrates differing by one methyl group is made possible by the presence of a hydrophobic pocket which can accommodate variable length apolar chains. This “hydrophobic continuum” also facilitates the alkyl transfer.

The high resolution of the determined structure allowed as many as 1600 water molecules to be modeled in the electron density. However, the active site contains only five of them, all of which are involved in cation coordination. As described below, at least one of these water molecules would be deprotonated and function in the isomerization process. In addition to those water mol-

ecules, the cations’ classical bipyramid coordination is completed by the carboxyl groups of acidic residues and three oxygen atoms of the inhibitor. Most of the conserved residues comprising regions I, II, III, IV, and V are involved in ligand binding (Figure 4). Region I corresponds to an  $\alpha$ -helix with a partial positive charge interacting with the negative charge of the diphosphate moiety of NADPH, as is usual for NAD(P)H-dependent dehydrogenases.<sup>24</sup> For region III, Glu319 interacts with one cation (Mn1), whereas Asp315 bridges both cations. Glu492 and Glu496 from region IV interact with only one cation (Mn2). Furthermore, Glu496 interacts with the part of the substrate that is involved in the alkyl transfer. Finally, Ser518 from region V stabilizes the carboxylate moiety of the substrate via two hydrogen bonds.

Although the crystallographic asymmetric unit contains four monomers, the active dimer is evident because of its extended interface area. These structural data are in agreement with gel filtration, equilibrium sedimentation experiments, and electrospray mass spectrometry, demonstrating that the spinach and barley enzymes are dimers.<sup>19,44,45</sup> The C-terminal domain is responsible for the entire dimer interface, which is mostly due to the plant-specific extra sequence residues 330–471 (Figure 3). This interface relies mostly on polar interactions (due to both side chains and  $\alpha$ -helical dipoles) and hydrophobic in-

teractions with one loop (residues 422–431) that extends toward the other monomer (Figure 3). Deletion of this loop converts the spinach enzyme from its normal dimeric form to a monomer and diminishes by about 200-fold its affinity for  $Mg^{2+}$ , to give a  $K_m$  of 1 mM.<sup>27</sup> This monomerization of the plant enzyme has no effect on the affinity for NADPH or for its substrates AL and AHB. The authors conclude from this work that the interactions between monomers have a long-range effect on the conformation of the  $Mg^{2+}$  binding sites, conferring on the plant enzyme its strong affinity for  $Mg^{2+}$ . Interestingly, the yeast enzyme, which naturally lacks this insert, has a low affinity for  $Mg^{2+}$  ( $K_m \approx 1$  mM) (Dumas, unpublished). The *E. coli* and *S. typhimurium* enzymes, which also contain a 140 amino acid supplementary sequence that is not homologous to that of the plant enzyme, have a low affinity for this metal ion.<sup>1,46</sup>

### Structural and Functional Comparisons with Other Enzymes

The fold of the C-terminal domain of the plant AHIR was unique when first described. However, because AHIR has a N-terminal domain with a classical Rossmann fold, its N-terminal domain shares strong similarities with the nucleotide binding domain of a number of NAD(P)H-dependent dehydrogenases such as glycerol 3-phosphate dehydrogenase.<sup>47</sup> Despite the high similarities between the 3-D structure of this domain of NAD(P)H-dependent dehydrogenases, it is interesting to point out that the similarity at the level of their amino acid sequence is very low and limited to the GXGXX(G/A)XXX(G/A) motif. Suresh et al.<sup>47</sup> have reported that there is a similarity to glycerol 3-phosphate dehydrogenase in the fold of the C-terminal domain.

AHIR belongs to the family of enzymes containing two catalytically active magnesium ions such as xylose isomerase<sup>48</sup> (PDB code 2GYI). Although the folding of the two enzymes is very different (xylose isomerase is an  $\alpha/\beta$ -barrel), the structures of the two proteins cocrystallized with two cations and a hydroxamate inhibitor disclose strong similarities at the level of their active sites.

Functional comparison of AHIR with other enzymes identifies 1-deoxy-D-xylulose 5-phosphate (DXP) reductoisomerase which, as its name suggests, catalyzes a reaction that parallels that of AHIR. This enzyme has come under intense scrutiny in the two years since it was first properly characterized.<sup>49,50</sup> Although it shows many catalytic similarities to AHIR, there is little, if any, sequence homology between the two enzymes. The reaction catalyzed forms part of the methylerythritol phosphate pathway for the biosynthesis of terpenoids. This pathway has an interesting parallel with that of branched-chain amino acid biosynthesis. The preceding enzyme (DXP synthase) requires thiamin diphosphate and catalyzes the decarboxylation of pyruvate followed by condensation with glyceraldehyde 3-phosphate.<sup>51</sup> The reaction prior to AHIR is that catalyzed by acetohydroxy acid synthase. This is another thiamin diphosphate-dependent enzyme and also

catalyzes the decarboxylation of pyruvate followed by a condensation, in this case with a 2-ketoacid.<sup>52</sup> Although the three-dimensional structures of neither DXP synthase nor acetohydroxy acid synthase have been determined, the structures of close relatives of each (transketolase and pyruvate oxidase, respectively) clearly show that the two enzymes share a common evolutionary heritage,<sup>53</sup> even though their sequence homology is all but obliterated.

### Order and Dynamic Studies of Ligand Binding

Kinetic experiments demonstrated that plant and bacterial AHIR obeys an ordered mechanism in which NADPH and  $Mg^{2+}$  bind first and independently, followed by substrate binding.<sup>1,19</sup> Later, the order and the stoichiometry of ligand binding were also demonstrated by electrospray mass spectrometry on the spinach enzyme.<sup>45</sup> The first evidence of conformational modifications of the plant AHIR upon ligand binding was obtained using the fluorescence properties of NADPH.<sup>19</sup> Addition of  $Mg^{2+}$  to the AHIR–NADPH complex leads to a small decrease of the emitted fluorescence, indicating that binding of the metal cofactor may trigger some conformational modifications. Furthermore, the emitted fluorescence of the AHIR–NADPH– $Mg^{2+}$  ternary complex was greatly modified upon addition of IpOHA (or Hoe 704), indicating that binding of the competitive inhibitor to the active site leads to further conformational changes. Another indicator of conformational changes came from crystallographic studies. The structure of the spinach enzyme cocrystallized with its cofactors and IpOHA shows that the inhibitor is completely buried inside the active site. This observation raises the question of how IpOHA can reach the active site and implies once again that conformational modifications occur during the binding process.

With a view to better characterizing the conformational influence of the ligands, hydrogen–deuterium exchange studies of the free enzyme and different complexes with  $Mg^{2+}$  and/or NADPH and/or the inhibitor IpOHA have been performed.<sup>54</sup> Each complex was digested using pepsin, and the resultant peptides were fractionated by HPLC and directly analyzed by electrospray ionization mass spectrometry (ESI-MS). Peptide sequences of non-deuterated peptic fragments were identified using both Edman degradation and tandem mass spectrometry. This experimental procedure allowed the accurate determination of the effect of each ligand on the accessibility of amide hydrogen atoms to solvent deuterium along the peptide backbone and provided a dynamic view of the ligand binding process (Figure 5). Magnesium ion was found to decrease deuterium accessibility at the level of region IV, at the interface of the N- and C-terminal domains and interestingly at the level of the N-terminal domain (Figure 4A). Similarly, NADPH binding leads to a mass decrease in peptides derived from both the NADPH domain and the C-terminal domain. Thus, binding of each cofactor leads to conformational modifications in the domain with which each interacts but also induces long-range modifications in the other domain. Binding of both

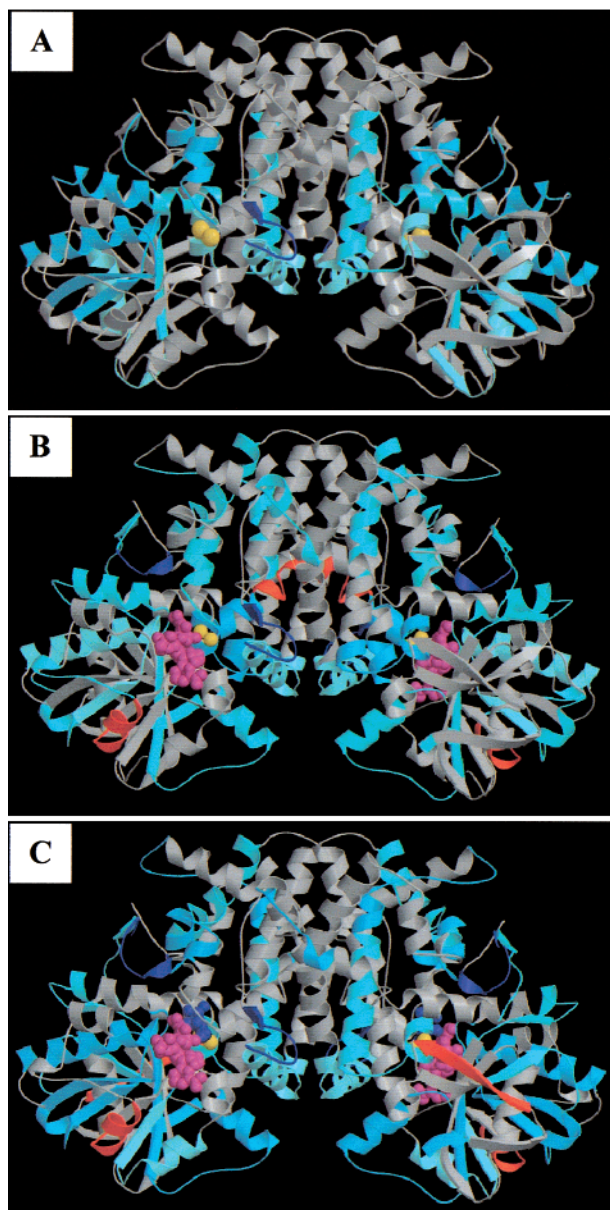


**FIGURE 5.** Conformational modifications of spinach AHIR upon ligand binding (redrawn from Halgand et al.<sup>54</sup>). The influence of (A)  $Mg^{2+}$  (yellow) alone, (B)  $Mg^{2+}$  and NADPH (pink), or (C)  $Mg^{2+}$ , NADPH, and the inhibitor IpOHA (blue) on the conformation of AHIR was determined by hydrogen–deuterium exchange mapping of peptic peptides. The graded shades of blue reflect the different levels of decrease of deuterium accessibility compared to the free enzyme, from small (10–20%, light blue) through medium (20–40%, medium blue) to large (40–60%, dark blue). Orange regions correspond to an increase in the level of deuterium incorporation upon ligand binding.

$Mg^{2+}$  and NADPH leads to a synergistic effect compared to the effect of each cofactor alone and also to a conformational change in region III (Figure 4B). Finally, binding of the inhibitor IpOHA to the enzyme complexed with  $Mg^{2+}$  and NADPH leads to a further decrease in solvent accessibility within the active site (Figure 4C). Interestingly, the deuterium accessibility of the loop involved in the dimerization is also affected greatly upon ligand binding, as  $Mg^{2+}$  ions and NADPH alone, together, or

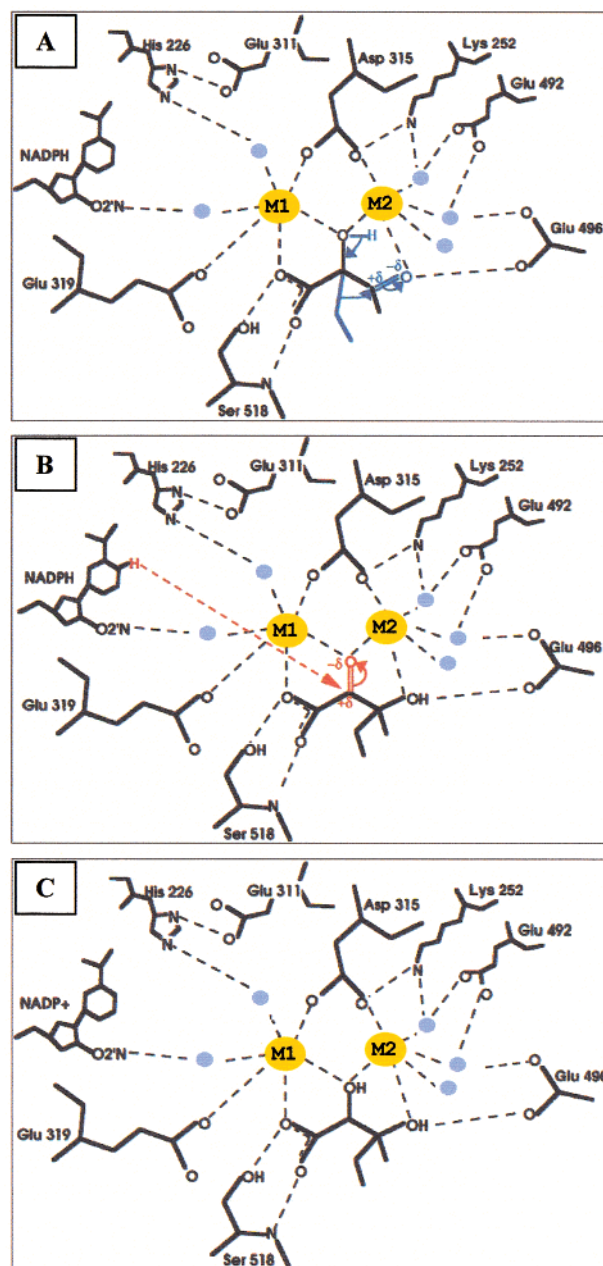


**FIGURE 6.** Proposal for the reaction mechanism of AHIR (redrawn from Thomazeau et al.<sup>25</sup>). An isomerization (A) followed by an NADPH-dependent reduction (B) leads to the reaction product (C); the figure describes the reaction with AHB as substrate. The blue and red regions show atoms involved in the isomerization or in the reduction, respectively. Pale blue filled circles correspond to water molecules. M1 and M2 correspond to the metal ions. See text for comments.

complexed with IpOHA induce a decrease in deuterium incorporation of about 50%. Thus, it appears that ligand binding induces not only a strong rigidity into the active site but also a stabilization of the dimer interface. The hydrogen–deuterium exchange experiments carried out on the spinach AHIR are in agreement with the proposed ordered mechanism and demonstrate that the conformation of the protein is dependent on the interactions with its ligands. These studies are a good illustration of the theory of “induced fit” proposed by Koshland and Neet,<sup>55</sup>



in which the binding of a cofactor and/or a substrate leads to conformational changes prior to the enzymatic reaction.

## Reaction Mechanism

The reaction mechanism of the plant AHIR has been studied using three complementary approaches: site-directed mutagenesis, crystallography, and molecular simulation. Based on site-directed mutagenesis, a first working model was proposed to account for the role of regions III and IV in catalysis.<sup>2</sup> The model proposes that regions III and IV function as the binding sites for the two magnesium ions that then act as Lewis acids to promote substrate isomerization and reaction intermediate reduction. Later, determination of the structure of the plant enzyme cocrystallized with IpOHA<sup>3</sup> or the reaction product dihydroxymethylvalerate<sup>25</sup> confirmed and clarified the proposed model. In the first step (Figure 6A), the isomerization reaction is initiated by the action of Mg<sup>2+</sup> (M2), which polarizes the carbonyl group on C3 of AHB, thus inducing a partial positive charge on C3. A hydroxyl group coordinated to Mg<sup>2+</sup> may participate in the rearrangement process by removing a proton from the hydroxyl group of the substrate. This deprotonation would be made easier by the two magnesium ions coordinated to the oxygen atom of the hydroxyl group of the substrate, thus increasing acidity of the corresponding proton. The transition state of the isomerization is thought to contain a transiently bridged alkyl function. In the reduction step, coordination of the reaction intermediate carbonyl by the two magnesium ions would polarize it, thus creating a partial positive charge on C2 and facilitating hydride transfer from NADPH (Figure 6B).

From these studies, we have now an idea of how the reaction proceeds. However, further experiments are needed to understand better this complex reaction. In particular, the function of a number of amino acids in the active site such as His226, Lys252, and Glu496 remains to be established (Figure 6). Also, the hydroxyl molecule involved in the deprotonation of the substrate in the initial stage of the isomerization remains to be identified. To gain more information on the reaction, theoretical simulation methods have been developed. Simulation of the first step of the reaction suggests that isomerization occurs almost simultaneously with a proton transfer from Glu496.<sup>56</sup> The initial events in the isomerization and the reduction step are currently being investigated.

## References

- Chunduru, S. K.; Mrachko, G. T.; Calvo, K. C. Mechanism of ketol acid reductoisomerase—steady-state analysis and metal ion requirement. *Biochemistry* **1989**, *28*, 486–493.
- Dumas, R.; Butikofer, M. C.; Job, D.; Douce, R. Evidence for two catalytically different magnesium-binding sites in acetohydroxy acid isomeroreductase by site-directed mutagenesis. *Biochemistry* **1995**, *34*, 6026–6036.
- Biou, V.; Dumas, R.; Cohen-Addad, C.; Douce, R.; Job, D.; Pebay-Peyroula, E. The crystal structure of plant acetohydroxy acid isomeroreductase complexed with NADPH, two magnesium ions and a herbicidal transition state analog determined at 1.65 Å resolution. *EMBO J.* **1997**, *16*, 3405–3415.
- Wek, R. C.; Hatfield, G. W. Nucleotide sequence and *in vivo* expression of the *ilvY* and *ilvC* genes in *Escherichia coli* K12. Transcription from divergent overlapping promoters. *J. Biol. Chem.* **1986**, *261*, 2441–2450.
- Wek, R. C.; Hatfield, G. W. Transcriptional activation at adjacent operators in the divergent-overlapping *ilvY* and *ilvC* promoters of *Escherichia coli*. *J. Mol. Biol.* **1988**, *203*, 643–663.
- Petersen, J. G. L.; Holmberg, S. The *ilv5* gene of *Saccharomyces cerevisiae* is highly expressed. *Nucleic Acids Res.* **1986**, *14*, 9631–9651.
- Dumas, R.; Joyard, J.; Douce, R. Purification and characterization of acetohydroxyacid reductoisomerase from spinach chloroplasts. *Biochem. J.* **1989**, *262*, 971–976.
- Dumas, R.; Lebrun, M.; Douce, R. Isolation, characterization and sequence analysis of a full-length cDNA clone encoding acetohydroxy acid reductoisomerase from spinach chloroplasts. *Biochem. J.* **1991**, *277*, 469–475.
- Dumas, R.; Curien, G.; DeRose, R. T.; Douce, R. Branched-chain-amino-acid biosynthesis in plants: molecular cloning and characterization of the gene encoding acetohydroxy acid isomeroreductase (ketol-acid reductoisomerase) from *Arabidopsis thaliana*. *Biochem. J.* **1993**, *294*, 821–828.
- Curien, G.; Dumas, R.; Douce, R. Nucleotide sequence and characterization of a cDNA encoding the acetohydroxy acid isomeroreductase from *Arabidopsis thaliana*. *Plant Mol. Biol.* **1993**, *21*, 717–722.
- Akhmanova, A.; Voncken, F. G.; Harhangi, H.; Hosea, K. M.; Vogels, G. D.; Hackstein, J. H. Cytosolic enzymes with a mitochondrial ancestry from the anaerobic chytrid *Piromyces* sp. E2. *Mol. Microbiol.* **1998**, *30*, 1017–1027.
- Zelenaya-Troitskaya, O.; Perlman, P. S.; Butov, R. A. An enzyme in yeast mitochondria that catalyzes a step in branched-chain amino acid biosynthesis also functions in mitochondrial DNA stability. *EMBO J.* **1995**, *14*, 3268–3276.
- Piatigorsky, J. Review: A case for corneal crystallins. *J. Ocul. Pharm. Therapeut.* **2000**, *16*, 173–180.
- Thompson-Coffe, C.; Borioli, G.; Zickler, D.; Rosa, A. L. Pyruvate decarboxylase filaments are associated with the cortical cytoskeleton of asci and spores over the sexual cycle of filamentous ascomycetes. *Fungal Genet. Biol.* **1999**, *26*, 71–80.
- Sirover, M. A. New insights into an old protein: The functional diversity of mammalian glyceraldehyde-3-phosphate dehydrogenase. *Biochim. Biophys. Acta* **1999**, *1432*, 159–184.
- Armstrong, F. B.; Hedgecock, C. J. R.; Reary, J. B.; Whitehouse, D.; Crout, D. H. G. Stereochemistry of the reductoisomerase and  $\alpha\beta$ -dihydroxyacid dehydratase-catalysed steps in valine and isoleucine biosynthesis. Observation of a novel tertiary ketol rearrangement. *J. Chem. Soc., Chem. Commun.* **1974**, 351–352.
- Armstrong, F. B.; Lipscomb, E. L.; Crout, D. H. G.; Mitchell, M. B.; Prakash, S. R. Biosynthesis of valine and isoleucine: synthesis and biological activity of (2S)- $\alpha$ -acetolactate acid (2-hydroxy-2-methyl-3-oxobutanoic acid), and (2R)- and (2S)- $\alpha$ -acetohydroxybutyric acid (2-ethyl-2-hydroxy-3-oxobutanoic acid). *J. Chem. Soc., Perkin Trans. 1* **1983**, 1197–1201.
- Hill, R. K.; Sawada, S.; Arfin, S. M. Stereochemistry of valine and isoleucine biosynthesis. IV. Synthesis, configuration, and enzymatic specificity of  $\alpha$ -acetolactate and  $\alpha$ -acetohydroxybutyrate. *Bioorg. Chem.* **1979**, *8*, 175–189.
- Dumas, R.; Job, D.; Ortholand, J. Y.; Emeric, G.; Greiner, A.; Douce, R. Isolation and kinetic properties of acetohydroxy acid isomeroreductase from spinach (*Spinacia oleracea*) chloroplasts overexpressed in *Escherichia coli*. *Biochem. J.* **1992**, *288*, 865–874.
- Arfin, S. M.; Umbarger, H. E. Purification and properties of the acetohydroxy acid isomeroreductase of *Salmonella typhimurium*. *J. Biol. Chem.* **1969**, *244*, 1118–1127.
- Umbarger, H. E. Evidence for a negative feedback mechanism in the biosynthesis of isoleucine. *Science* **1956**, *123*, 848.
- Biou, V.; Pebay-Peyroula, E.; Cohen-Addad, C.; Vives, F.; Butikofer, M.-C.; Curien, G.; Job, D.; Douce, R.; Dumas, R. Biosynthesis of branched-chain amino acids in plants: structure and function of acetohydroxy acid isomeroreductase. In *Photosynthesis: from light to biosphere*; Mathis P., Ed.; Kluwer: Dordrecht, 1995; Vol. V, pp 335–340.
- Rane, M. J.; Calvo, K. C. Reversal of the nucleotide specificity of ketol acid reductoisomerase by site-directed mutagenesis identifies the NADPH binding site. *Arch. Biochem. Biophys.* **1997**, *338*, 83–89.
- Wierenga, R. K.; De Maeyer, M. C. H.; Hol, W. G. Interaction of pyrophosphate moieties with alpha-helices in dinucleotide binding-proteins. *Biochemistry* **1985**, *24*, 1346–1357.

- (25) Thomazeau, K.; Dumas, R.; Halgand, F.; Forest, E.; Douce, R.; Biou, V. Structure of spinach acetohydroxyacid isomeroreductase complexed with its reaction product dihydroxymethylvalerate, manganese and (phospho)-ADP-ribose. *Acta Crystallogr. D* **2000**, *56*, 389–397.
- (26) Dumas, R.; Biou, V.; Douce, R. Purification and characterization of a fusion protein of plant acetohydroxy acid synthase and acetohydroxy acid isomeroreductase. *FEBS Lett.* **1997**, *408*, 156–160.
- (27) Wessel, P. M.; Biou, V.; Douce, R.; Dumas, R. A loop deletion in the plant acetohydroxy acid isomeroreductase homodimer generates an active monomer with reduced stability and altered magnesium affinity. *Biochemistry* **1998**, *37*, 12753–12760.
- (28) Donadini, R.; Copeland, L. Acetohydroxy acid reductoisomerase of wheat. *Aust. J. Plant Physiol.* **2000**, *27*, 417–423.
- (29) Primerano, D. A.; Burns, R. O. Role of acetohydroxy acid isomeroreductase in biosynthesis of pantothenic acid in *Salmonella typhimurium*. *J. Bacteriol.* **1983**, *153*, 259–269.
- (30) Hill, C. M.; Duggleby, R. G. Purified recombinant *Escherichia coli* ketol-acid reductoisomerase is unsuitable for use in a coupled assay of acetohydroxyacid synthase activity due to an unexpected side reaction. *Protein Expression Purif.* **1999**, *15*, 57–61.
- (31) Shimizu, S.; Kataoka, M.; Chung, M. C.; Yamada, H. Ketopantoic acid reductase of *Pseudomonas maltophilia* 845. Purification, characterization, and role in pantothenate biosynthesis. *J. Biol. Chem.* **1988**, *263*, 12077–12084.
- (32) Julliard, J. H. Purification and characterization of oxopantoilactone reductase from higher plants—role in pantothenate synthesis. *Bot. Acta* **1994**, *107*, 191–200.
- (33) Shematek, E. M.; Diven, W. F.; Arfin, S. M. Subunit structure of  $\alpha$ -acetohydroxy acid isomeroreductase from *Salmonella typhimurium*. *Arch. Biochem. Biophys.* **1973**, *158*, 126–131.
- (34) Schulz, A.; Sponemann, P.; Kocher, H.; Wengenmayer, F. The herbicidally active experimental compound Hoe 704 is a potent inhibitor of the enzyme acetolactate reductoisomerase. *FEBS Lett.* **1988**, *238*, 375–378.
- (35) Aulabaugh, A.; Schloss, J. V. Oxalyl hydroxamates as reaction-intermediate analogues for ketol-acid reductoisomerase. *Biochemistry* **1990**, *29*, 2824–2830.
- (36) Dumas, R.; Cornillon-Bertrand, C.; Guigue-Talet, P.; Genix, P.; Douce, R.; Job, D. Interactions of plant acetohydroxy acid isomeroreductase with reaction intermediate analogues: correlation of the slow, competitive, inhibition kinetics of enzyme activity and herbicidal effects. *Biochem. J.* **1994**, *301*, 813–820.
- (37) Dumas, R.; Vives, F.; Job, D.; Douce, R.; Biou, V.; Pebay-Peyroula, E.; Cohen-Addad, C. Inhibition of acetohydroxy acid isomeroreductase by reaction intermediate analogues: herbicidal effect, kinetic analysis and 3-D structural studies. *Brighton Crop Protection Conference—Weeds 1995*; British Crop Protection Council: Farnham, UK, 1995; Vol. 7B-3, pp 833–842.
- (38) Halgand, F.; Vives, F.; Dumas, R.; Biou, V.; Andersen, J.; Andrieu, J. P.; Cantegril, R.; Gagnon, J.; Douce, R.; Forest, E.; Job, D. Kinetic and mass spectrometric analyses of the interactions between plant acetohydroxy acid isomeroreductase and thiadiazole derivatives. *Biochemistry* **1998**, *37*, 4773–4781.
- (39) Gouet, P.; Courcelle, E.; Stuart, D. I.; Metz, F. ESPript: analysis of multiple sequence alignments in PostScript. *Bioinformatics* **1999**, *15*, 305–308.
- (40) Henikoff, J. G.; Henikoff, S. Blocks database and its applications. *Methods Enzymol.* **1996**, *266*, 88–105.
- (41) Kabsch, W.; Sander, C. Dictionary of protein secondary structure: pattern recognition of hydrogen-bonded and geometrical features. *Biopolymers* **1983**, *22*, 2577–2637.
- (42) Dumas, R.; Job, D.; Douce, R.; Pebay-Peyroula, E.; Cohen-Addad, C. Crystallization and preliminary crystallographic data for acetohydroxy acid isomeroreductase from *Spinacia oleracea*. *J. Mol. Biol.* **1994**, *242*, 578–581.
- (43) Taylor, W. R. A deeply knotted protein structure and how it might fold. *Nature* **2000**, *406*, 916–919.
- (44) Durner, J.; Knörzer, O. C.; Böger, P. Ketol-acid reductoisomerase from barley (*Hordeum vulgare*). Purification, properties, and specific inhibition. *Plant Physiol.* **1993**, *103*, 903–910.
- (45) Laprèvote, O.; Serani, L.; Das, B. C.; Halgand, F.; Forest, E.; Dumas, R. Stepwise building of a 115-kDa macromolecular edifice monitored by electrospray mass spectrometry. The case of acetohydroxy acid isomeroreductase. *Eur. J. Biochem.* **1999**, *256*, 356–359.
- (46) Hoffer, J. G.; Decedue, C. J.; Luginbuhl, G. H.; Reynolds, J. A.; Burns, R. O. The subunit structure of  $\alpha$ -acetohydroxyacid isomeroreductase from *Salmonella typhimurium*. *J. Biol. Chem.* **1975**, *250*, 877–882.
- (47) Suresh, S.; Turley, S.; Opperdoes, F. R.; Michels, P. A.; Hol, W. G. A potential target enzyme for trypanocidal drugs revealed by the crystal structure of NAD-dependent glycerol-3-phosphate dehydrogenase from *Leishmania mexicana*. *Structure Fold. Des.* **2000**, *8*, 541–552.
- (48) Lavie, A.; Allen, K. N.; Petsko, G. A.; Ringe, D. X-ray crystallographic structures of D-xylose isomerase-substrate complexes position the substrate and provide evidence for metal movement during catalysis. *Biochemistry* **1994**, *33*, 5469–5480.
- (49) Takahashi, S.; Kuzuyama, T.; Watanabe, H.; Seto, H. A 1-deoxy-D-xylulose 5-phosphate reductoisomerase catalyzing the formation of 2-C-methyl-D-erythritol 4-phosphate in an alternative nonmevalonate pathway for terpenoid biosynthesis. *Proc. Natl. Acad. Sci. U.S.A.* **1998**, *95*, 9879–9884.
- (50) Proteau, P. J.; Woo, Y. H.; Williamson, R. T.; Phaosiri, C. Stereochemistry of the reduction step mediated by recombinant 1-deoxy-D-xylulose 5-phosphate isomeroreductase. *Org. Lett.* **1999**, *1*, 921–923.
- (51) Rohmer, M.; Seemann, M.; Horbach, S.; Bringer-Meyer, S.; Sahm, H. Glyceraldehyde 3-phosphate and pyruvate as precursors of isoprenic units in an alternative non-mevalonate pathway for terpenoid biosynthesis. *J. Am. Chem. Soc.* **1996**, *118*, 2564–2566.
- (52) Duggleby, R. G.; Pang, S. S. Acetohydroxyacid synthase. *J. Biochem. Mol. Biol.* **2000**, *33*, 1–36.
- (53) Muller, Y. A.; Lindqvist, Y.; Furey, W.; Schulz, G. E.; Jordan, F.; Schneider, G. A thiamin diphosphate binding fold revealed by comparison of the crystal-structures of transketolase, pyruvate oxidase and pyruvate decarboxylase. *Structure* **1993**, *1*, 95–103.
- (54) Halgand, F.; Dumas, R.; Biou, V.; Andrieu, J. P.; Thomazeau, K.; Gagnon, J.; Douce, R.; Forest, E. Characterization of the conformational changes of acetohydroxy acid isomeroreductase induced by the binding of  $Mg^{2+}$  ions, NADPH, and a competitive inhibitor. *Biochemistry* **1999**, *38*, 6025–6034.
- (55) Koshland, D. E.; Neet, K. E. The catalytic and regulatory properties of enzymes. *Annu. Rev. Biochem.* **1968**, *37*, 359–410.
- (56) Proust-De Martin, F.; Dumas, R.; Field, M. J. A hybrid-potential free-energy study of the isomerization step of the acetohydroxy acid isomeroreductase reaction. *J. Am. Chem. Soc.* **2000**, *122*, 7688–7697.

AR000082W